

REVIEWER #1

General comments:

This is a generally well written manuscript on the retrieval of tropospheric ozone within convective clouds retrieved from UV nadir observations with the OMI instrument complemented by MLS observations of stratospheric ozone. I think the manuscript should eventually be published, but there are several aspects that should first be addressed in my opinion.

The approach used to determine what is called “cloud ozone” is quite pragmatic. This is not necessarily a problem, but the limitations of the applied method are not discussed in sufficient detail in my opinion.

A problem with validating the OMI/MLS cloud ozone is lack of independent ozone measurements for deep convective clouds. The Ziemke et al. (2009) paper was a predecessor to the current paper and included validation and discussions of limitations of the cloud ozone measurements and also included RT model calculations of vertical sensitivity of ozone in deep convective clouds. The Strode et al. (2017) paper (currently in review and listed in the references) is a related side study. Strode et al. (2017) tests the validity of the OMI/MLS residual cloud ozone measurements against a free-running chemistry climate model (CCM). The CCM is found to simulate key features of both the cloudy-clear differences and the geographic distribution of the in-cloud ozone from OMI/MLS. In our study we include an anonymous ftp site for the cloud ozone data. We look forward to getting feedback from other researchers on the usefulness and quality of these measurements from their analyses.

It is stated several times that the derived cloud ozone corresponds to the average O₃ VMR inside the cloud. However, the nadir measurements are probably very insensitive to O₃ in the lower or middle part of a convective cloud, i.e. the retrieved O₃ VMR reflects O₃ in the upper part of the cloud and does that in a non-trivial way, probably. In this respect it would be very valuable to determine and/or show a measure of the sensitivity of the retrieval to O₃ at different levels below cloud top. Perhaps you have already done sensitivity studies like that for earlier papers?

I’m also wondering how different the cloud penetration depths at the wavelengths used for the OCP and the O₃ retrievals are. The wavelengths are quite close, so the difference is probably not too large, but it may affect the results in a non-trivial way.

I’m also wondering, what the effect of light-path enhancements due to multiple scattering inside the clouds on the O₃ retrievals is? The RT is quite complex in this case and I’m not sure, whether this complexity can simply be neglected.

It is mentioned several times that the OCP is deep within the cloud (several 100 hPa below the actual cloud top). This surprises me and I wonder, whether this is expected. Have you performed simulations of the RT inside the cloud? The fact that OCPs are

well below the cloud top suggests that a large fraction of the UV photons can penetrate the cloud deeply. I'm not sure this is expected. Perhaps I'm missing a point here. Please add more information here and, if available, mention or cite studies that deal with this complex RT problem.

You have very valid comments above regarding the issue of UV penetration in thick clouds. We have actually done a considerable amount of work on addressing the issues that you mention above with several papers listed in the references. The Vasilkov et al. (2008), Ziemke et al. (2009), and Joiner et al. (2012) papers may be the most detailed and included a comprehensive RT code that includes the effects of multiple scattering within clouds (denoted LIDORT-RRS). We discuss these papers including the Vasilkov et al. (2008) paper further below pertaining to your comments.

You often use the term "above-cloud column", which is misleading, because the column in the paper actually also includes the ozone in the top part of the clouds. I suggest using another term or at least emphasizing this point explicitly in the paper.

In section 2 (third paragraph) we had mentioned in a sentence that we refer to the "cloud ozone" as the ozone column or mean VMR lying between the OMI OCP and the tropopause. In our revision right after that sentence we now add that we refer to "above-cloud ozone" as the column ozone measured from the top of the atmosphere down to the OMI OCP. We double checked to make sure that we didn't accidentally type "above-cloud ozone" for "cloud ozone" (or vice versa) in the paper.

I would like to point out that my intention is not to ask you to do a lot of RT simulations (perhaps you have already done so, though) to address the issues raised above, but rather to discuss these aspects openly (you've probably thought about all of them, and perhaps they are not that important), and to discuss the limitations of the method and the results.

Specific comments:

Line 56: "Huntreiser" -> "Huntrieser"

Done.

Line 123: "As shown by Vasilkov et al. (2008), the OCP at UV wavelengths lies deep inside the clouds, often by several hundred hPa and therefore is not a measure of true cloud top;" I'm surprised that the OCP is so much below the cloud top at UV. Is this expected based on the approach to estimate cloud top pressure using the OMI UV radiances?

Thanks for the comment – this is an important property of the UV measurements. In section 2 and in the references we included several papers by Joiner and Bhartia (1995), Joiner et al. (2004), Joiner and Vasilkov (2006), Vasilkov et al. (2008), Ziemke et al. (2009), and Joiner et al. (2012) on this subject. In the revision we added the

Joiner et al. (2012) paper as it is more recent than the others. The papers by Vasilkov et al. (2008), Ziemke et al. (2009), and Joiner et al. (2012) used a Linearized Discrete-Ordinate Radiative Transfer RRS (LIDORT-RRS) code (Spurr et al., 2007) for calculations. They studied sensitivity to geometrical cloud thicknesses and included CloudSat reflectivity profiles and MODIS IR cloud pressures. They describe the large differences (up to several hundred hPa) between physical cloud top and OCP measured by OMI using their OMCLDRR algorithm. Below is Figure 12 adapted from the Vasilkov et al. (2008) paper that illustrates this result:

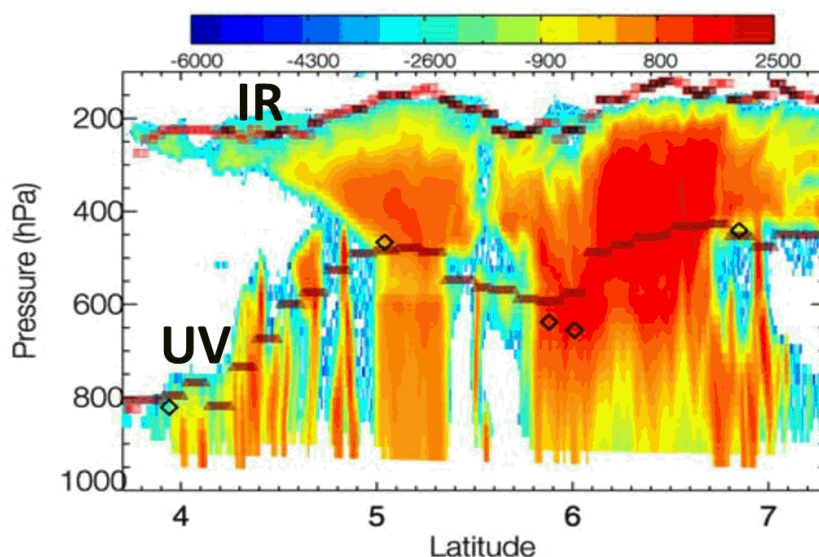


Figure 12. Cloudsat radar reflectivity on 13 November 2006 with cloud pressures retrieved from OMCLDRR (rust triangle curves, denoted UV), retrieved from MODIS (top red squares, denoted IR), and simulated for OMI on the basis of CloudSat/MODIS data (black diamonds).

The Ziemke et al. (2009) and Joiner et al. (2012) papers listed in the references and main text also involved further LIDORT-RRS calculations. The Joiner et al. (2012) paper describes a fast simulator to compute the OCP quickly from profiles of optical extinction such as from models or CloudSat/MODIS.

Line 137: “for bright clouds”. What about clouds that are not “bright”? I’m wondering how one would distinguish between bright clouds and the other ones. Do you only use bright clouds in this study?

We only used bright cloud scenes to derive all of the cloud ozone measurements – the bright cloud scenes for the residual and ensemble methods both used only OMI scenes with radiative cloud fraction greater than 80%.

Line 140: I find the term “cloud ozone” somewhat misleading, because it certainly does not correspond to the entire ozone column inside the cloud. The OCP will generally be

well above the cloud bottom and the “cloud ozone” will then correspond only to a fraction of the column ozone actually inside the cloud.

You are correct that we don’t measure ozone mean VMR for the entire thick cloud but instead between the tropopause and OMI OCP. In section 2 we mentioned that the “cloud ozone” from OMI/MLS refers to the ozone mean VMR lying between the OCP and tropopause. We have now also added in the revision that “above-cloud ozone” refers to the column ozone from the top of the atmosphere down to the OCP measured by OMI.

Line 147: “OMI above-cloud column ozone”. This also includes the “cloud ozone”, right? I think this should be mentioned explicitly, because for the inexperienced reader this is not obvious, and it may suggest that there are different OMI ozone column data products.

This is related to the previous comment where we added the definition for above-cloud ozone which should help clarify the discussion in this paragraph.

Line 162: “With SCO representing column ozone from the top of the atmosphere down to the tropopause, all tropospheric ozone measurements in our analyses are independent of any stratospheric ozone barring possible unresolved stratospheric intrusions and unknown errors.” I don’t agree with this statement. An important aspect is the (limited) vertical resolution of the MLS ozone profiles. MLS will not be able to retrieve the true vertical variation of ozone, but the measurement process corresponds to (roughly speaking) the convolution of the true vertical ozone profile with the MLS O3 averaging kernels, which will have a width of several km. This means, that some of the stratospheric O3 may (or rather will) be smeared into the troposphere. This effect will probably be on the order of at least several DU, potentially significantly more. Perhaps this aspect has been addressed in previous studies already?

Very good point... The MLS v4.2 data quality document shows that the vertical resolution for MLS about the tropopause is ~3 km which will affect the quality of the cloud ozone measurements from OMI/MLS. In the revision we have deleted those sentences and replaced with new ones mentioning inherent errors in SCO from both NCEP tropopause pressure and MLS retrieval errors (esp. vertical sensitivity about the tropopause).

Figure 1, line 592: “For deep convective cumulonimbus clouds the cloud tops are near the tropopause and so the mean volume mixing ratio is primarily a measurement of average “in-cloud” ozone concentration.” I don’t think this statement is correct. I agree that for well developed clouds one can assume that their tops are close to the tropopause, but the fraction of the measured column below cloud top will certainly not correspond to the average ozone amount inside the cloud, right? Your measurement will be rather insensitive to the amount of ozone in the lower part of the cloud. It would be interesting to know what the mean penetration depth of UV radiation at around 350 nm inside optically thick clouds is.

This relates to the comments above for Line 140 including RT calculations by Vasilkov et al., (2008).

Figure 1: y-axis label of the inset: “above cloud column ozone”. I think this is misleading (or I’m missing the point), because this ozone columns includes your “cloud ozone”, right?

Thanks – we have revised the Figure 1 caption and discussion to clarify this point.

Line 182: “above cloud column ozone“. See last comment.

Relating to previous comment.

Line 192: Effective scene pressure. I’m wondering, whether it would be better to determine an effective scene altitude, rather than pressure. But if you use only cases with $f > 0.8$ this probably does not make a big difference. Perhaps there was a specific reason to use pressure here?

We chose to use pressure since the OMI ozone algorithm and measurements are based on vertical pressure coordinate. Other instruments like OMPS or SAGE as examples measure number density as a function of altitude – for those measurements it may be more advantageous to use altitude rather than pressure.

Line 197: “In our case for deep convective cumulonimbus clouds the cloud tops are near tropopause level and so the derived mixing ratio is primarily an average measurement of ozone inside the clouds.” As mentioned above, I don’t think this is true. I think the derived mixing ratio is some sort of average over a part of the cloud, and it’s probably non-trivial to determine what part of the cloud this actually is. Again, if you know what the estimated penetration depth is, this would be a useful piece of information. Also, as mentioned above, the light-path enhancement due to multiple scattering will affect the sensitivity of the measurements to ozone inside the cloud.

It is difficult to quantify the penetration depth relative to actual physical cloud top. To get cloud-top information we need to use other ancillary cloud measurements that have different view times and are not properly co-located. Making 1-1 evaluations even more difficult is that these clouds including their cloud properties can change relatively quickly on time scales of just ~10-15 minutes. Having UV and IR sensors on the same spacecraft and with near-equivalent sample times would be nearly ideal for getting at coincident OCP and IR cloud tops and estimated penetration depth. Actually, what is really needed is a combination of an imager like MODIS and CloudSat to provide optical depth profiles. For OMI measurements we filter thick clouds for OCPs < 550 hPa and anticipate (as suggested in the figure above from Vasilkov et al.) that these are generally optically thick clouds with physical tops near the tropopause. In previous papers we addressed multiple scattering including multiple cloud decks (also illustrated

in this same figure at the far left) – resulting errors are largely reduced from the RCF and OCP filtering that we apply to the scene data.

Line 253: “theses” -> “these”

Done.

Line 628: “OCP’s” -> “OCPs”

Done.

Figures 8 and 9: I’m not sure, how robust the differences between background and cloud ozone really are. I accept that the clear sky values are probably very realistic average tropospheric O₃ VMRs, but I’m not sure the cloud ozone is really a good measurement for the O₃ VMR inside the cloud. There must be differences – perhaps small – in the penetration depths at the wavelengths used for the O₃ retrieval and the OCP retrieval. This may lead to systematic errors. And I’m not sure, whether the light-path enhancements inside the cloud are compensated entirely by using the OCP retrievals for reference. These aspects should be commented upon, I think. The paper is still interesting, but I think the limitations of the technique should be stated. And if all of these potential problems are well understood – i.e. no limitations – this should also be mentioned.

Differences between the clear and cloudy ozone time series in Figures 8-9 are definitely robust in terms of sheer magnitudes and seasonal variability. These differences seem to make sense under hypothesis of injection of (high to low) concentrations of boundary layer ozone upward into the clouds. You also mention about the differences of penetration depths between the retrievals for ozone and OCP. It turns out that the difference is about 317-330 nm for ozone and 350 nm for OCP. Most of the scattering inside the clouds is from cloud particles and not from Rayleigh. Our simulations show only small differences in photon path versus wavelength. In the referenced papers we evaluated such potential errors/limitations as you have mentioned above. As note, there are going to be systematic errors, both regional and temporal in nature with the cloud ozone measurements due to so many parameters involved. These include errors in retrieved OMI OCP and column ozone, errors with MLS ozone profiles, and errors in tropopause pressure from the NCEP re-analyses. Quantifying systematic errors for even just one of these quantities is extremely difficult and likely not possible to accomplish with useful degree of accuracy.

REVIEWER #2

General Comments:

This paper describes a long-term record of monthly mean cloud ozone in the tropics derived from OMI/MLS measurements. It is derived from the residual between OMI

ozone above convective clouds and MLS stratospheric ozone. As the OMI cloud pressure is often in the middle of clouds and the physical cloud tops often reach the tropopause, the derived residual ozone generally therefore represents ozone inside clouds, difficult to be measured otherwise. The OMI/MLS cloud ozone is also compared with cloud ozone derived from OMI alone using the ensemble cloud slicing. The spatiotemporal distribution of cloud ozone is discussed in contrast with background ozone. The analysis shows persistent low ozone in the tropical Pacific and higher ozone over landmass regions and connections with ENSO, intra-seasonal/Madden-Julian oscillation variability and boundary layer pollution. This study is suitable for publication in AMT. It is well logically organized. Overall, I recommend it to be published after addressing the following minor comments.

Specific Comments:

1. L115, do you mean OMI V3 as V8.5 is for the OMTO3 algorithm not for all OMI products

We now inserted a sentence to clarify that v8.5 is the actual retrieval algorithm for the OMI ozone.

2. L251, the sentence “The panels in Figure 4 : : : ozone (asterisks)” is redundant with the first sentence and can be removed.

We had a typo – the parentheses in the first sentence should have been singular stating as “panel” rather than “panels”. The third sentence states that OMI/MLS residual cloud ozone is represented by the thick curve and ensemble cloud ozone is represented by the asterisk curve in each of the two panels.

3. L267-269, you may add something to explain the larger uncertainty, e.g., due to the sparseness of clouds as indicated by much fewer derived ensemble cloud ozone in this region

Done.

4. Last paragraph of section 3, is the OMI/MLS cloud ozone product derived on the daily basis? If not, mention monthly mean and the grid cell for averaging. Briefly mention that it is limited to 30S-30N and explain why.

These are excellent points... We have now clarified the use of daily measurements that were then averaged monthly in the first paragraph, and also the final two paragraphs that describe the OMI ensemble method and OMI/MLS residual method. We mention at the end of section 3 why we limited to 30S-30N regarding noise issues.

5. L286-290, please mention the enhanced ozone over the Pacific/Atlantic Ocean at latitude closer to 30S/30N.

Good point. We have now included discussion of the observed cloud ozone concentrations over ocean in this paragraph.

6. L292, it is good to define “background” here, i.e., by adding “(near clear-sky scenes with radiative cloud fractions less than 30%)”

Another good point... Done.

7. In last paragraph of section 5, is it contradictory between saying “STE accounts for <5% of ozone over tropical Atlantic” around L299 and “stratospheric ozone contribution is the most important factor for driving the IAV of upper tropospheric ozone : : :” around L308? Please clarify it.

Thanks for catching this – although both Sauvage et al. (2007) and Liu et al. (2017) examined the tropospheric ozone over the tropical Atlantic, Sauvage et al. (2007) focused on the source contribution of tropospheric annual-averaged ozone budget. In contrast the Liu et al. (2017) conclusion was focused on the source contribution of ozone IAV during the austral winter season in the middle and upper troposphere, of which there are large ozone changes due to STE. We have rewritten the text to make this clear.

8. In Figure 8 and L335-345, it is useful to add correlation between aerosol index and cloud ozone over Southern Africa

Done.

9. L356-360, any other speculation for the relatively low cloud ozone around 2010-2012?

It could instead be related partly to ENSO decadal variability (e.g. Nino 3.4 plotted in following Figure 9 for the east Pacific) but that is also speculation. We would really need a longer record and a comprehensive stratosphere-troposphere photochemical transport model to attempt to explain.

A Cloud-Ozone Data Product from Aura OMI and MLS Satellite Measurements

Jerald R. Ziemke^{1,2}, Sarah A. Strode^{2,3}, Anne R. Douglass², Joanna Joiner², Alexander Vasilkov^{2,4}, Luke D. Oman², Junhua Liu^{2,3}, Susan E. Strahan^{2,3}, Pawan K. Bhartia², David P. Haffner^{2,4}

¹Morgan State University, Baltimore, Maryland, USA

²NASA Goddard Space Flight Center, Greenbelt, Maryland, USA

³Universities Space Research Association, Columbia, MD, USA

⁴SSAI, Lanham, Maryland, USA

Abstract. Ozone within deep convective clouds is controlled by several factors involving photochemical reactions and transport. Gas-phase photochemical reactions, and heterogeneous surface chemical reactions involving ice, water particles, and aerosols inside the clouds all contribute to the distribution and net production and loss of ozone. Ozone in clouds is also dependent on convective transport that carries low troposphere/boundary layer ozone and ozone precursors upward into the clouds. Characterizing ozone in thick clouds is an important step for quantifying relationships of ozone with tropospheric H₂O, OH production, and cloud microphysics/transport properties. Although measuring ozone in deep convective clouds from either aircraft or balloon ozonesondes is largely impossible due to extreme meteorological conditions associated with these clouds, it is possible to estimate ozone in thick clouds using backscattered solar UV radiation measured by satellite instruments. Our study combines Aura Ozone Monitoring Instrument (OMI) and Microwave Limb Sounder (MLS) satellite measurements to generate a new research product of monthly-mean ozone concentrations in deep convective clouds between 30°S to 30°N for October 2004 – April 2016. These measurements represent mean ozone concentration primarily in the upper levels of thick clouds and reveal key features of cloud ozone including: persistent low ozone concentrations in the tropical Pacific of ~10 ppbv or less; concentrations of up to 60 ppbv or greater over landmass regions of South America, southern Africa, Australia, and India/east Asia; connections with tropical ENSO events; and intra-seasonal/Madden-Julian Oscillation variability. Analysis of OMI aerosol measurements suggests a cause and effect relation between boundary layer pollution and

elevated ozone inside thick clouds over land-mass regions including southern Africa and India/east Asia.

1. Introduction.

Measuring tropospheric ozone in deep convective clouds including convective outflow regions in the mid-upper troposphere is important for several reasons. Ozone in the upper troposphere is a major greenhouse gas that contributes to climate forcing. The IPCC 2013 Report (e.g., in Hartmann et al., 2014; <http://www.ipcc.ch/report/ar5/wg1/>) includes an evaluation of tropospheric versus stratospheric ozone using a collage of radiative transfer model calculations. The report shows that the radiative forcing of tropospheric ozone is 10 times greater than that of stratospheric ozone, even though only 10% of the atmospheric ozone resides in the troposphere. The IPCC 2013 report (and references therein) also notes that ozone is a major surface pollutant, and is important as the main source of OH, the primary cleanser of pollutants in the troposphere. Measurements of ozone associated with deep convection are needed to characterize the extent of ozone inter-relationships with tropospheric H₂O and OH production, and in understanding cloud microphysics/transport properties and resulting influence on global and regional tropospheric ozone distributions.

Microphysics and photochemistry can be very complex for deep convective clouds. Huntrieser et al. (2016, and references therein) combined aircraft and cloud measurements with a model to study ozone distributions and sources associated with deep convective clouds over the central U.S. Huntrieser et al. (2016) identified upward transport of lower tropospheric ozone and ozone precursors into the upper troposphere within thick clouds. They also showed that cloud tops over-shoot the tropopause and inject high amounts of biomass burning pollutants (largely CO and NO_x) and lightning-produced NO_x into the low stratosphere, while at the same time ozone-rich air from the low stratosphere is transported downward into the cloud anvil and surrounding outflow regions as a dynamical response to overshooting. Some of the Geostationary Operational Environmental Satellite (GOES) cloud tops were found to reach up to 17-18 km altitude for these deep convective systems. Pronounced ozone-rich stratospheric air was observed within cloud outflow regions.

The ozonesonde measurement record includes occurrences of very low to even “near-zero” ozone concentrations in the tropical upper troposphere associated with the passing of deep convective cloud systems (e.g., Kley et al., 1996; Folkins et al., 2002; Solomon et al., 2005). The very low ozone values are largely attributed to convective lifting of low concentrations of ozone from the marine boundary layer into the upper troposphere. In pollution-free oceanic regions it is not uncommon for ozone in the marine boundary layer to be only a few ppbv due to ozone net loss reactions involving hydrogen radicals OH and HO₂ (e.g., Solomon et al., 2005, and references therein). Some studies suggest the possibility of in-cloud photochemical ozone destruction mechanisms (e.g., Zhu et al., 2001; Barth et al., 2002; Liu et al., 2006). Vömel and Diaz (2010) showed that improperly calibrated Electrochemical Concentration Cell (ECC) ozonesondes led to a small measurement error (under-determination) and the near-zero upper troposphere ozone concentrations reported in these studies. Vömel and Diaz (2010) found that the near-zero ozone concentrations in the upper troposphere were instead about 10 ppbv and attributed the calibration error to unaccounted variations associated with background cell currents at launch. Vömel and Diaz (2010) indicate that the studies measuring “near-zero” ozone were not wrong, but instead slightly underdetermined the low ozone concentrations.

The very low ozone measurements in the tropical upper troposphere in past studies were obtained from a limited number of aircraft flights and ozonesondes at a few isolated sites in the vicinity of, but not inside, deep convective cloud systems. Measuring ozone directly inside deep convective clouds from ozonesondes and aircraft instruments remains an elusive task due to extreme meteorological conditions associated with the clouds. Ziemke et al. (2009) developed a residual “cloud slicing” method for measuring ozone volume mixing ratios within thick clouds by combining Aura Ozone Monitoring Instrument (OMI) and Microwave Limb Sounder (MLS) satellite measurements. For deep convective clouds, OMI provided the tropospheric cloud ozone measurements after subtracting co-located MLS stratospheric column ozone. Their study found large variability in the ozone concentrations in thick clouds. While very low ozone concentrations (< 10 ppbv) in the clouds were identified in the remote Indian and Pacific Ocean regions, concentrations greater than 60 ppbv were obtained over continental landmasses including Africa. Ziemke et al. (2009) hypothesized that the ozone measured in thick clouds is

largely a manifestation of ozone concentrations (from low to high amounts) present in the low troposphere/boundary layer that become transported upward by convection.

We build upon the cloud slicing work of Ziemke et al. (2009) to produce a long data record of OMI/MLS cloud ozone measurements as that former study was limited to only a few months **during** 2005 and 2006. As with Ziemke et al. (2009), we derive ozone mixing ratios inside tropical deep convective clouds by combining Aura OMI measurements of total column ozone and cloud pressure with Aura MLS stratospheric column ozone. **The ozone measurements represent mean ozone concentrations in the upper levels of the clouds above 550 hPa.** This paper is organized as follows: Section 2 details the satellite measurements while Section 3 is an overview of cloud slicing. Section 4 discusses validation and Sections 5-6 discuss basic characteristics and scientific interpretations of the data. Finally, Section 7 provides a summary.

2. Satellite Measurements.

Our study combines Aura OMI and MLS ozone measurements with OMI aerosols and cloud parameters (i.e., cloud pressures, radiative cloud fractions). OMI is a UV/VIS solar backscatter spectrometer that makes daily measurements of Earth radiances and solar irradiances from 270 to 500 nm with spectral resolution of about 0.5 nm (Levelt et al., 2006). OMI scans perpendicular to the orbit path with 60 side-scan positions and provides near-global coverage of the sunlit Earth with a pixel size of 13 km \times 24 km at nadir. **The current OMI total ozone that we use is derived using a v8.5 algorithm.** Description and access to the OMI v8.5 data can be obtained from the website <http://disc.sci.gsfc.nasa.gov/Aura/data-holdings/OMI>. In January 2009 a physical external optical blockage known as the “row anomaly” reduced the number of the 60 good side-scanning row measurements to about 30-40. Scan positions 21-55 are the most affected, with dependence on latitude and specific day. All of the OMI measurements that we use were properly screened to exclude all data affected by the row anomaly artifact.

OMI cloud pressures and radiative cloud fractions are derived using UV-2 radiances (Vasilkov et al., 2008). The cloud pressure from OMI is named optical centroid pressure (OCP). As shown by Vasilkov et al. (2008), the OCP at UV wavelengths lies deep inside the clouds, often by

several hundred hPa and therefore is not a measure of true cloud top; they showed this by comparing the OMI OCP measurements with both Cloudsat radar reflectivity profiles and MODIS IR cloud pressures. The OCP effectively represents the bottom reflecting surface for the OMI retrievals in the presence of clouds. The true ozone measurement from OMI is the column amount from the top of the atmosphere down to the reflecting surface. In the presence of a cloud, the OMI algorithm places an ozone “ghost column” climatology estimate below the OCP reflecting surface to obtain total column ozone.

There are two OMI algorithms that determine the OCP. The first algorithm is based on O₂-O₂ dimer absorption (Sneep et al., 2008) and the second is based on rotational-Raman scattering (RRS) that uses spectral structures in the ratio of backscattered radiance to solar irradiance, known as the Ring effect (Joiner and Bhartia, 1995; Joiner et al., 2004; Joiner and Vasilkov, 2006, Joiner et al., 2012). The two OMI cloud algorithms provide similar estimates of OCP for bright clouds although there are small differences due to algorithmic and physical effects (Sneep et al., 2008). We use the RRS cloud pressure for our study although our results would be nearly identical using the O₂-O₂ cloud measurements. We refer to “cloud ozone” as the ozone column or ozone mean volume mixing ratio lying between the tropopause and retrieved OCP from OMI under conditions of deep convection. We also refer to “above-cloud ozone” as the ozone column measured from OMI lying from the top of the atmosphere down to the OMI OCP. Deep convective clouds often have cloud tops at or near the tropopause. Therefore much if not most of the tropospheric ozone measured between the tropopause and OMI cloud pressure lie within the cloud itself rather than above the cloud top.

Aura MLS v4.2 profile ozone is included to measure fields of stratospheric column ozone (SCO). MLS SCO is used in conjunction with OMI above-cloud column ozone each day to derive mean column amounts and mean concentrations of ozone measured over deep convective clouds. The MLS ozone profiles are vertically integrated in log-pressure from 0.0215 hPa down to the tropopause to derive measurements of SCO as described by Ziemke et al. (2006, 2009). To separate stratospheric from tropospheric ozone we similarly use the WMO 2K-km⁻¹ lapse-rate tropopause pressure definition with NCEP re-analysis temperatures. Other tropopause pressure definitions and other meteorological analyses besides NCEP could have also been used. We

included the WMO definition with NCEP for both historical reasons and consistency checking relative to previous versions of our OMI/MLS tropospheric ozone products that used the same NCEP tropopause. For the low latitudes in our study we expect that there would be only minor differences in our results if we used instead a different tropopause. All MLS v4.2 retrieval quality flags (quality, status, convergence, and precision) are properly adhered to for all of our analyses. The MLS v4.2 measurements including data quality and quality flags are described in the MLS data quality document http://mls.jpl.nasa.gov/data/v4-2_data_quality_document.pdf. Recommended pressure levels for science applications with MLS v4.2 ozone are 0.0215 hPa to 261 hPa. There are errors in derived SCO from MLS caused by both errors in NCEP tropopause pressure and MLS data themselves. The MLS v4.2 data quality document indicates that the vertical resolution for MLS about the tropopause is about 3 km. For daily SCO this can affect these measurements by adding errors of several DU. In our study we average all daily measurements over a month to derive cloud ozone which will reduce these errors if truly random.

3. Overview of Cloud Slicing.

We use two cloud slicing methods to measure cloud ozone from Aura OMI and MLS instruments. The first method is called “ensemble” cloud slicing that uses daily co-located measurements of cloud pressure and column ozone. This algorithm was first proposed by Ziemke et al. (2001) and combined co-located Nimbus-7 TOMS column ozone and THIR IR cloud-top pressure. Here we combine OMI column ozone with OMI cloud pressure (i.e., OCP). An advantage of ensemble cloud ozone is that it requires only a single instrument, but weaknesses are noisiness and poor spatial resolution in the measurements. The second method is a residual cloud slicing approach (Ziemke et al., 2009) that combines OCPs from OMI with residual column ozone differences between OMI and MLS. An advantage of the residual method is that it can yield measurements with high horizontal resolution. The cloud ozone product that we generate comes from the OMI/MLS residual method. We use OMI ensemble measurements only as a consistency check for the OMI/MLS residual ozone.

A schematic diagram for the ensemble cloud slicing method is shown in Figure 1. A region is first chosen (top of figure, $5^\circ \times 5^\circ$ region shown) with all coincident measurements (either daily

or daily measurements accumulated over a month) of OMI above-cloud column ozone plotted versus OCP effective cloud pressure (bottom of figure). The OCP as noted in Section 2 may lie several hundred hPa below the cloud top, and the OMI algorithm places a climatological ozone ghost column below the OCP to determine total column ozone. For cloud slicing we use only the above-cloud ozone from OMI which is the true measurement. In practice, we determine the above-cloud column ozone by subtracting the ghost column ozone from total column ozone reported in the OMI level-2 orbital datasets.

In Figure 1 the OMI footprint scene depicted is 100% cloud filled so that the OCP deep inside the cloud represents the bottom reflecting surface for the OMI retrieval. In the more general case, footprint scenes from OMI will not be 100% cloud filled and we account for this. What we actually use for cloud slicing in the Figure 1 schematic is an effective scene pressure (P_{EFF}) in place of the OCP. P_{EFF} is derived from $P_{EFF} = P_{CLOUD} \cdot f + P_{SURFACE} \cdot (1 - f)$, where P_{CLOUD} is the cloud OCP, $P_{SURFACE}$ is the Earth surface scene pressure, and f is the OMI scene radiative cloud fraction (Joiner et al., 2009). We use OMI measurements for cloud slicing only when radiative cloud fraction f is greater than 0.80. When f is equal to 1.0 the calculated P_{EFF} is equivalent to OCP. In our case for deep convective cumulonimbus clouds the cloud tops are near tropopause level and so the derived mixing ratio is primarily an average measurement of ozone inside the clouds.

Tropospheric ozone mean volume mixing ratio (VMR) is estimated by fitting a straight line to the data pairs of above-cloud column ozone versus OCP over the selected geographical region. This method was first described by Ziemke et al. (2001) and is summarized here. Column ozone ($\Delta\Omega$) between two altitudes z_1 and z_2 is by definition the number of molecules per unit horizontal area and is calculated by integrating ozone number density n as $\Delta\Omega = \int_{z_1}^{z_2} n \cdot dz$. Using hydrostatic balance $\partial P / \partial z = -\rho g$ (ρ is mass density, g is acceleration of gravity) and assuming an invariant acceleration of gravity for the troposphere this expression can be converted to: $\Delta\Omega$ (in Dobson Units, DU; $1 \text{ DU} = 2.69 \times 10^{20} \text{ molecules-m}^{-2}$) = $C \cdot \int_{P_1}^{P_2} X \cdot dP = C \cdot \bar{X} \cdot (P_2 - P_1)$, where $C = 0.00079 \text{ DU-hPa}^{-1}\text{-ppbv}^{-1}$ and \bar{X} is ozone mean VMR in units ppbv. It follows that

ozone mean VMR in the troposphere is \bar{X} (ppbv) = $1270 \cdot \Delta\Omega / \Delta P$, or in other words 1270 multiplied by the slope of the ensemble line fit. The 2σ uncertainty for VMR in ppbv is determined by multiplying the calculated 2σ uncertainty of the slope by 1270. An estimate for SCO can also be obtained by extrapolating the line fit to the mean tropopause pressure over the region. The above-cloud ozone at the extrapolated tropopause pressure, a direct estimate of SCO, can be compared with MLS SCO to assess how well the ensemble method separates stratospheric from tropospheric column ozone.

An example of ensemble scatter plots is shown in Figure 2 for October 5, 2008. The left scatter plot coincides with the region of southern Africa while the right scatter plot coincides with the western Pacific. Measured ozone mixing ratio is 72 ppbv over southern Africa and 10 ppbv over the western Pacific. The enhanced ozone over southern Africa suggests that ozone produced from regional pollution including biomass burning, which is largest around September-October each year in the SH, reaches the upper regions of the clouds. However, the regional elevated ozone over southern Africa may be caused by other sources including lightning NO_x , and transport by the Walker circulation, and mixing of stratospheric air that is transported into the troposphere in response to cloud tops overshooting the tropopause (e.g., Huntrieser et al., 2016, and references therein). The low ozone VMR in the western Pacific in Figure 2 is consistent with low values measured in the vicinity of tropical deep convection by ozonesondes (e.g., Kley et al., 1996; Folkins et al., 2002; Solomon et al., 2005; Vömel and Diaz, 2010). **In principle we derive monthly cloud ozone measurements instead of daily from the ensemble method by accumulating all co-located daily data pairs over a month.**

Figure 3 illustrates the residual technique for measuring cloud ozone. This method combines OMI above-cloud column ozone and OMI OCP with MLS SCO. **All of these combined measurements are daily and are co-located.** For a deep convective cloud the OCP lies well inside the cloud with a cloud top often at or near the tropopause, so that much or most of measured tropospheric ozone lies inside the cloud rather than above the cloud top. The relationship (Joiner et al., 2009) to derive residual cloud ozone VMR (units ppbv) is $\text{VMR} = 1270 \cdot [\Delta\Omega / (P_{\text{EFF}} - P_{\text{TROPOPAUSE}})]$, where $\Delta\Omega$ is the difference (in DU) of OMI above-

cloud column ozone minus MLS SCO, $P_{TROPopause}$ is tropopause pressure (in hPa), and P_{EFF} is the effective scene pressure (also in hPa) as defined above. The number 1270 is the same as for the ensemble method to ensure units ppbv for VMR. **As a final step, monthly-mean residual values are derived from the daily residual measurements.**

We limit the latitude range for both the ensemble and residual methods to 30° S - 30° N. This was done for both approaches to reduce inherent noise due in part to strong dynamical variability of the tropopause from the tropospheric wind jets.

4. OMI/MLS Residual Cloud Ozone Product: Validation and Consistency Checks.

The validation of OMI/MLS residual cloud ozone measurements is not straightforward given the paucity of in-cloud measurements from independent sources such as ozonesondes and aircraft. However, as one approach similar to Ziemke et al. (2009), we can still obtain at least a consistency check between the OMI/MLS residual cloud ozone and cloud ozone obtained from the OMI-only ensemble method.

Figure 4 compares cloud ozone from the ensemble and residual techniques for July 2015 (left panel) and October 2015 (right panel). Both of these months coincide with the intense 2014-2016 El Nino. The **two** panels in Figure 4 **each** compare OMI/MLS residual cloud ozone (thick curves) and OMI ensemble cloud ozone (asterisks). The 5°S-10°N latitude band was chosen because it includes much of the ITCZ with thick clouds for these months. Both the ensemble and residual cloud ozone in Figure 4 are low to near zero in the eastern and western Pacific close to the dateline; it is conceivable that these oceanic regions coincide generally with pristine air and low concentrations of both ozone and ozone precursors in the boundary layer. In contrast, over a broad region extending from the western Pacific to Indonesia the cloud ozone from both measurements is enhanced. The increased tropospheric ozone is due to a combination of suppressed convection during El Nino and increases in biomass burning over Sumatra and Borneo due to the induced dry conditions and wildfires (e.g., Chandra et al., 1998; Logan et al., 2008). The suppressed convection during El Nino coincides with reduced upward injection of low ozone concentrations in the oceanic boundary layer compared to non-El Nino years, thus

contributing to anomalous increase in cloud ozone relative to non-ENSO years. In the central Atlantic the cloud ozone measurements are ~ 50 ppbv for both methods indicating higher ozone concentrations injected into the clouds from below and in general a more polluted region compared to the Pacific. In the eastern Atlantic extending to the Indian Ocean / western Pacific (i.e., $\sim 60^\circ$ – 120°) the ensemble measurements are larger than for OMI/MLS. The calculated $\pm 2\sigma$ uncertainties for the ensemble measurements are large everywhere including this broad region and illustrate the noisy nature of the ensemble method **due largely to sparseness of thick clouds**. Unlike measurements for the OMI/MLS residual method, large errors in ozone for the ensemble method may originate largely from the basic assumptions of the methodology such as uniformity of both SCO and tropospheric mixing ratio throughout the chosen region. In the next two sections we discuss the OMI/MLS cloud ozone product for basic geophysical characteristics including some science results.

5. Monthly Distributions.

Figure 5 shows monthly-mean climatology maps of OMI/MLS residual cloud ozone derived from averaging similar months over the long record. Plotted in Figure 5 is mean VMR (units ppbv) representing average ozone concentration lying between the tropopause and OMI OCP as described in Section 3. In Figure 5 the mean mixing ratio is calculated for OCPs varying between 250 hPa and 550 hPa. The black regions in the figure indicate not enough deep convective clouds present and/or mostly clouds such as low-marine stratus clouds with OCP lying below the 550 hPa threshold.

The distributions in Figure 5 illustrate the large regional and temporal variability present in cloud-ozone. In the remote Pacific and Indian Ocean regions the values of cloud ozone are small at ~ 10 ppbv or less. High values reaching 70-80 ppbv are measured for landmass regions of India/east Asia, southern Africa and South America, and Australia. The high ozone is indicative of a more polluted lower troposphere/boundary layer. **There are also some ozone values ~ 40 -50 ppbv over both the Atlantic and Pacific Ocean regions in higher latitudes which are large yet still small compared to the noted high values over landmasses.** Understanding variations in the ozone

concentrations over oceanic thick clouds is work in progress that combines these OMI/MLS measurements with a free-running chemistry-climate model (Strode et al., 2017).

Figure 6 shows climatology maps similar to Figure 5 but instead for “background” ozone mean VMR. The background ozone is derived using only OMI near clear-sky scenes for column ozone where radiative cloud fractions are less than 30%. In Figure 6 the east-west tropical wave-1 pattern in tropospheric ozone (Fishman et al., 1990) is easily discerned year round with high values ~60-80 ppbv in the Atlantic and low values ~20 ppbv in the eastern and western Pacific. According to Sauvage et al. (2007) using the GEOS-Chem Chemical Transport Model (CTM) the main source of tropospheric ozone in the tropical Atlantic on annual-mean basis comes from lightning NO_x with smaller contributions from biomass burning, soils, and fossil fuels (by factors varying ~4-6). Their CTM also indicated that stratosphere-troposphere exchange (STE) accounts for less than about 5% of tropospheric ozone burden in the tropical Atlantic and that most of the effects from NO_x came from Africa. In the SH subtropics in Figure 6 there is a buildup of high ozone in August-November along all longitudes. Although the SH Atlantic maximum in Figure 6 occurs in every month year round, this feature also exhibits substantial inter-annual variability. Liu et al. (2017) combined GEOS-5 assimilated OMI/MLS ozone and Goddard Modeling Initiative (GMI) CTM simulations to quantify the causes of the inter-annual variability (IAV) of tropospheric ozone over four sub-regions of the southern hemispheric tropospheric ozone maximum. They found that the strong influence of emission on ozone IAV is largely confined to the South Atlantic region in September at and below ~430 hPa. In the middle and upper troposphere, the IAV of the stratospheric ozone contribution is the most important factor driving the IAV of ozone over two selected tropical regions: the tropical south Atlantic and tropical S. E. Pacific, especially during the austral winter season.

6. Time Series.

With about 12 years of measurements from OMI/MLS we can analyze variability from monthly to decadal timescales of the OMI/MLS residual cloud ozone and compare these changes with background ozone. In Figure 7 we show eight selected regions of interest for background ozone (top) and cloud ozone (bottom) for October 2006. For these eight selected regions we have

averaged cloud ozone and background ozone each month to generate long-record time series starting October 2004.

Time series of the monthly background ozone and cloud ozone for the eight regions are plotted in Figures 8 and 9. In all of these eight panels the background ozone is plotted as the thick solid curve while cloud ozone is the thin curve with asterisks. Also plotted for the six landmass regions in Figures 8-9 are time series of the OMI aerosol index (dotted blue curves). In Figure 8 for northern Africa we include a line plot of the solar MgII UV index (blue squares) for comparing decadal changes in ozone in all eight panels in Figures 8-9 with the 11-year solar cycle. In the eastern Pacific region in Figure 9 the Nino 3.4 index (blue squares) is also plotted to demonstrate the dependence of cloud ozone variability from ENSO in this particular region. All background ozone and aerosol time series in Figures 8-9 were flagged missing wherever (at $1^\circ \times 1.25^\circ$ gridding) and whenever (monthly means) corresponding measurements for cloud ozone were missing.

Figure 8 compares ozone time series for the following four regions: Central America, South America, northern Africa, and southern Africa. **In each panel the correlation between cloud ozone and background ozone is shown. In addition the correlation between cloud ozone and aerosols is also included for southern Africa.** With the exception of the southern Africa region, the background ozone is larger than cloud ozone by ~ 10 - 20 ppbv year round. For southern Africa the cloud ozone each year in summer months exceeds background ozone by ~ 5 - 10 ppbv on average. The annual cycle for cloud ozone with southern Africa does not appear to be in phase with background ozone, reaching its annual maximum about 1-2 months earlier. The aerosol index time series in Figure 8 for southern Africa represents seasonality of biomass burning in the region and it also peaks 1-2 months prior to maximum background ozone; **the correlation between cloud ozone and aerosols shown in this panel for southern Africa is about 0.63.** Sporadic thick clouds in the presence of tropospheric ozone from biomass burning via nearby regions may explain the higher ozone values and 1-2 month phase lead for cloud ozone relative to background ozone.

With Central America in Figure 8 (upper left panel) some of the month-to-month maxima and minima for cloud ozone coincide with relative maxima and minima in background ozone on intra-seasonal time scale. The Central America region including the Caribbean Sea/Gulf of Mexico and extending into the tropical north Atlantic is well documented for intra-seasonal variability in winds and cyclonic development (e.g., Park and Schubert, 1993; Maloney and Hartmann, 2000; Mo, 2000; Foltz and McPhaden, 2004, 2005). Seasonal variability in Figure 8 for both background ozone and cloud ozone is most pronounced for southern Africa and weakest for northern Africa.

For decadal time scale, the background ozone in all four regions in Figure 8 is mostly invariant while cloud ozone shows small decreases toward the middle of the record followed by small increases afterward. Comparing with the MgII index in the upper right panel, this decadal variability for cloud ozone does not appear to be directly related to the 11-year cycle in solar UV which has minima centered around year 2009 and also at the end of the record.

Figure 9 shows time series for four additional regions: India/east Asia, Indonesia, eastern Pacific, and Australia. With the exception of Australia (lower right panel), the background ozone is larger than cloud ozone by ~10-20 ppbv year round. The cloud ozone and background ozone for Australia are comparable during July-November months (i.e., similar to southern Africa in Figure 8). For Indonesia and the eastern Pacific the cloud ozone is sometimes very low to even near zero which is indicative of clean air with low concentrations of boundary-layer ozone and ozone precursors. Indonesia in Figure 9 indicates intra-seasonal variability for both cloud ozone and background ozone. In this western pacific region the main source of intra-seasonal variability of tropospheric ozone is the 1-2 month Madden-Julian Oscillation (e.g., Ziemke et al., 2015, and references therein).

Decadal changes of cloud ozone in Figure 9, with the exception of the eastern Pacific, appears again to have relative minima around the middle of the long record and no clear connection with the 11-year solar cycle in UV. Included in the panel for the eastern Pacific region is the Nino 3.4 index time series (squares along bottom) which was re-scaled for plotting with the ozone. For the eastern Pacific it is clear that there is dominant inter-annual variability related to ENSO

events with associated changes in convection/SST (i.e., opposite correlation between them is indicated). For this eastern Pacific region the cloud ozone is greatest during La Nina (suppressed convection in the region) and lowest during El Nino (enhanced convection in the region).

It is difficult to discern timing of the seasonal minima and maxima of the aerosol and ozone time series in Figures 8-9. For this reason we have included Figure 10 that compares 12-month climatologies of background ozone, cloud ozone, and aerosol index time series for the six landmass regions plotted in Figures 8-9. One main conclusion from Figure 10 is that seasonal maxima of background ozone for the landmass regions of southern Africa, India/east Asia, and Australia all tend to occur about one month after maxima in aerosols. For southern Africa and India/east Asia the aerosol maximum occurs around the same month as the maximum in cloud ozone. These phase shifts suggest that biomass burning during the mostly dry season has an important impact on the seasonal cycles of tropospheric ozone including India where monsoon does not generally begin until late May or early June. It is beyond the scope of our study to explain the relative amplitude differences and phase shifts between background and cloud ozone measurements. Explaining these characteristics will require a future investigation using either a chemical transport model or a chemistry-climate model with an appropriate convection scheme.

7. Summary.

We applied a residual technique to derive a data record (October 2004-recent) of tropospheric ozone mixing ratios inside deep convective clouds in the tropics and subtropics from OMI/MLS satellite measurements. This residual technique makes use of the cloud optical centroid pressure (OCP) obtained from the effects of rotational-Raman scattering in the OMI UV spectra. Solar UV penetrates deep into thick clouds, often by several hundred hPa. In addition, deep convective clouds have high cloud tops often near or at tropopause level. As a result the OMI/MLS cloud ozone measurements are largely indicative of ozone concentrations lying inside the clouds.

The OMI/MLS residual cloud ozone was compared with OMI/MLS near clear-sky ozone (denoted “background” ozone) indicating substantially lower concentrations (by ~10-20 ppbv)

for cloud ozone year round, with the exception of southern Africa and Australia during July-November months. For both southern Africa and Australia the seasonal maxima of cloud ozone was found to exceed seasonal maxima of background ozone by about 5-10 ppbv. For both southern Africa and India/east Asia the seasonal maxima for both OMI aerosols and cloud ozone occurs about 1-2 months earlier than for background ozone. The analyses imply a cause and effect relation between boundary layer pollution and elevated ozone inside thick clouds over land-mass regions including southern Africa and India/east Asia.

While large cloud ozone concentrations ~60 ppbv or greater occur over landmass regions of India/east Asia, South America, southern Africa, and Australia, very low cloud ozone is persistent over the Indian Ocean and eastern/western Pacific Ocean with values ~10 ppbv or smaller. A low concentration of cloud ozone measured in these oceanic regions is indicative of generally pristine air with small amounts of ozone and ozone precursors in the marine boundary layer/low troposphere.

There is indication of intra-seasonal variability in cloud ozone over the eastern and western Pacific Ocean regions and also over Central America. In the western Pacific the intra-seasonal variability originates largely from the 1-2 month Madden-Julian Oscillation. In the eastern Pacific the largest variability is inter-annual and originates from ENSO and associated changes in SST/convection. In the eastern Pacific the highest cloud ozone occurs during La Nina (suppressed convection over the region) with lowest cloud ozone during El Nino (enhanced convection).

Understanding changes in convection versus changes in emissions and how they relate to the variabilities in measured cloud ozone is beyond the scope of our study. A photochemical model involving deep convective clouds would be necessary to study the variability for cloud ozone from monthly to decadal time scale. Strode et al. (2017) is current work in progress that combines these OMI/MLS measurements with a chemistry-climate model to evaluate properties of cloudy versus clear-sky background ozone.

The monthly gridded cloud ozone and background ozone data can be obtained via anonymous ftp from the following:

```
> ftp jwocky.gsfc.nasa.gov  
> Name: anonymous  
> Password: (your email address)  
> cd pub/ccd/data_monthly  
> get vmr_30s_to_30n_oct04_to_apr16.sav
```

Acknowledgments. The authors thank the Aura MLS and OMI instrument and algorithm teams for the extensive satellite measurements used in this study. OMI is a Dutch-Finnish contribution to the Aura mission. Funding for this research was provided in part by NASA NNH14ZDA001N-DSCOVr.

References.

Barth, M. C., P. G. Hess, and S. Madronich, Effect of marine boundary layer clouds on tropospheric chemistry as analyzed in a regional chemistry transport model, J. Geophys. Res., 107, (D11), 4126, 2002.

Chandra, S., J. R. Ziemke, W. Min, and W. G. Read, Effects of 1997-1998 El Nino on tropospheric ozone and water vapor, Geophys. Res. Lett., 25, 3867-3870, 1998.

Fishman, J., C. E. Watson, J. C. Larsen, and J. A. Logan, Distribution of tropospheric ozone determined from satellite data, *J. Geophys. Res.*, 95(D4), 3599-3617, 1990.

Folkens, I., C. Braun, A. M. Thompson, and J. Witte, Tropical ozone as an indicator of deep convection, *J. Geophys. Res.*, 107 (D13), doi:10.1029/2001JD001178, 2002.

Foltz, G. R., and M. J. McPhaden, The 30–70 day oscillations in the tropical Atlantic, *Geophys. Res. Lett.*, 31, L15205, doi:10.1029/2004GL020023, 2004.

Foltz, G. R., and M. J. McPhaden, Mixed layer heat balance on intra-seasonal time scales in the northwestern tropical Atlantic Ocean, *J. Clim.*, 18(20), 4168 – 4187, 2005.

Hartmann, D. L., A. M. G. Klein Tank, M. Rusticucci, L. V. Alexander, S. Brönnimann, Y. Charabi, F. J. Dentener, E. J. Dlugokencky, D. R. Easterling, A. Kaplan, B. J. Soden, P. W. Thorne, M. Wild and P. M. Zhai, Observations: Atmosphere and Surface. In: *Climate Change 2013: The Physical Science Basis. Contribution of Working Group I to the Fifth Assessment Report of the Intergovernmental Panel on Climate Change* [Stocker, T. F., D. Qin, G.-K. Plattner, M. Tignor, S. K. Allen, J. Boschung, A. Nauels, Y. Xia, V. Bex, and P.M. Midgley (eds.)], Cambridge University Press, Cambridge, United Kingdom and New York, NY, USA, 2014.

Huntrieser, H., et al., On the origin of pronounced O₃ gradients in the thunderstorm outflow region during DC3, *J. Geophys. Res. Atmos.*, 121, 6600–6637, doi:10.1002/2015JD024279, 2016.

Joiner J., and P. K. Bhartia, The determination of cloud pressures from rotational-Raman scattering in satellite backscatter ultraviolet measurements. *J. Geophys. Res.*, 100, 23,019-23,026, 1995.

Joiner, J., A. P. Vasilkov, D. E. Flittner, J. F. Gleason, and P. K. Bhartia, Retrieval of cloud pressure and oceanic chlorophyll content using Raman scattering in GOME ultraviolet spectra, *J. Geophys. Res.*, 109, D01109, doi:10.1029/2003JD003698, 2004.

Joiner, J., and A. P. Vasilkov, First results from the OMI rotational Raman scattering cloud pressure algorithm, *IEEE Trans. Geosci. Rem. Sens.*, 44, 1272-1282, 2006.

Joiner, J., M. R. Schoeberl, A. P. Vasilkov, L. Oreopoulos, S. Platnick, N. J. Livesey, and P. F. Levelt (2009), Accurate satellite-derived estimates of the tropospheric ozone impact on the global radiation budget, *Atmos. Chem. Phys.*, 9, 4447-4465, doi:10.5194/acp-9-4447-2009.

Joiner, J., A. P. Vasilkov, P. Gupta, P. K. Bhartia, P. Veefkind, M. Sneep, J. de Haan, I. Polonsky, and R. Spurr, Fast simulators for satellite cloud optical centroid pressure retrievals; evaluation of OMI cloud retrievals, *Atmos. Meas. Tech.*, 5, 529-545, doi:10.5194/amt-5-529-2012, 2012.

Kley, D., P. J. Crutzen, H. G. J. Smit, et. al. (1996), Observations of near-zero ozone concentrations over the convective Pacific: Effects on air chemistry, *Science*, 274, 230-233.

Levelt, P. F., et al., The Ozone Monitoring Instrument, *IEEE Trans. Geophys. Remote Sens.*, 44(5), 1093-1101, 2006.

Liu, H. Y., J. H. Crawford, R. B. Pierce, et al., Radiative effect of clouds on tropospheric chemistry in a global three-dimensional chemical transport model, *J. Geophys. Res.*, 111 (D20), D20303, 2006.

Liu, J. J. M. Rodriguez, S. D. Steenrod, A. R. Douglass, J. A. Logan, M. A. Olsen, K. Wargan, and J. R. Ziemke, Causes of interannual variability over the southern hemispheric tropospheric ozone maximum, *Atmos. Chem. Phys.*, 17, 3279-3299, doi:10.5194/acp-17-3279-2017, 2017.

Logan, J. A., I. Megretskaya, R. Nassar, et al., Effects of the 2006 El Niño on tropospheric composition as revealed by data from the Tropospheric Emission Spectrometer (TES), *Geophys. Res. Lett.*, 35, L03816, 2008.

Maloney, E. D., and D. L. Hartmann, Modulation of hurricane activity in the Gulf of Mexico by the Madden-Julian Oscillation, *Science*, 287, 2002 – 2004, 2000.

Mo, K. C., The association between intra-seasonal oscillations and tropical storms in the Atlantic Basin, *Mon. Weather Rev.*, 128, 4097–4107, 2000.

Park, C.-K., and S. D. Schubert, Remotely forced intra-seasonal oscillations over the tropical Atlantic, *J. Atmos. Sci.*, 50, 89 – 103, 1993.

Sauvage, B., R. V. Martin, A. van Donkelaar, and J. R. Ziemke, Quantification of the factors controlling tropical tropospheric ozone and the South Atlantic maximum, *J. Geophys. Res.*, 112 (D11) D11309, doi:10.1029/2006JD008008, 2007.

Solomon, S., D. W. J. Thompson, R. W. Portmann, et al., On the distribution of and variability of ozone in the tropical upper troposphere: Implications for tropical deep convection and chemical-dynamical coupling, *Geophys. Res. Lett.*, 32, L23813, doi:10.1029/2005GL024323, 2005.

Sneep, M., J. De Haan, P. Stammes, P. Wang, C. Vanbaume, J. Joiner, A. Vasilkov, and P. Levelt, Three way comparison between OMI/Aura and POLDER/PARASOL cloud pressure products, *J. Geophys. Res.*, doi:10.1029/2007JD008694, 2008.

Strode, S. A., A. R. Douglass, J. R. Ziemke, M. Manyin, J. E. Nielsen, and L. D. Oman, Analysis of ozone in clear versus cloudy conditions, *J. Geophys. Res.*, in review, 2017.

Vasilkov, A., J. Joiner, R. Spurr, et al., Evaluation of the OMI cloud pressures derived from rotational Raman scattering by comparisons with other satellite data and radiative transfer simulations, *J. Geophys. Res.*, 113, D15S19, doi:10.1029/2007JD008689, 2008.

Vömel, H., and K. Diaz, Ozone sonde cell current measurements and implications for observations of near-zero ozone concentrations in the tropical upper troposphere, *Atmos. Meas. Tech.*, 3, 495505, doi:10.5194/amt-3-495-2010, 2010.

Zhu, B., H. Xiao, M. Huang, and Z. Li, Numerical study of cloud effects on tropospheric ozone, *Water, Air, and Soil Pollution*, 129, 199-216, 2001.

Ziemke, J. R., S. Chandra, and P. K. Bhartia, "Cloud slicing": A new technique to derive upper tropospheric ozone from satellite measurements, *J. Geophys. Res.*, 106, 9853-9867, 2001.

Ziemke, J. R., S. Chandra, B. N. Duncan, et al., Tropospheric ozone determined from Aura OMI and MLS: Evaluation of measurements and comparison with the Global Modeling Initiative's Chemical Transport Model, *J. Geophys. Res.*, 111, D19303, doi:10.1029/2006JD007089, 2006.

Ziemke, J. R., J. Joiner, S. Chandra, P. K. Bhartia, A. Vasilkov, D. P. Haffner, K. Yang, M. R. Schoeberl, L. Froidevaux, and P. F. Levelt, Ozone mixing ratios inside tropical deep convective clouds from OMI satellite measurements, *Atmos. Chem. Phys.*, 9, 573-583, 2009.

Ziemke, J. R., A. R. Douglass, L. D. Oman, S. E. Strahan, and B. N. Duncan, Tropospheric ozone variability in the tropical Pacific from ENSO to MJO and shorter timescales, *Atmos. Chem. Phys.*, 15, 8037-8049, doi:10.5194/acp-15-8037-2015, 2015.

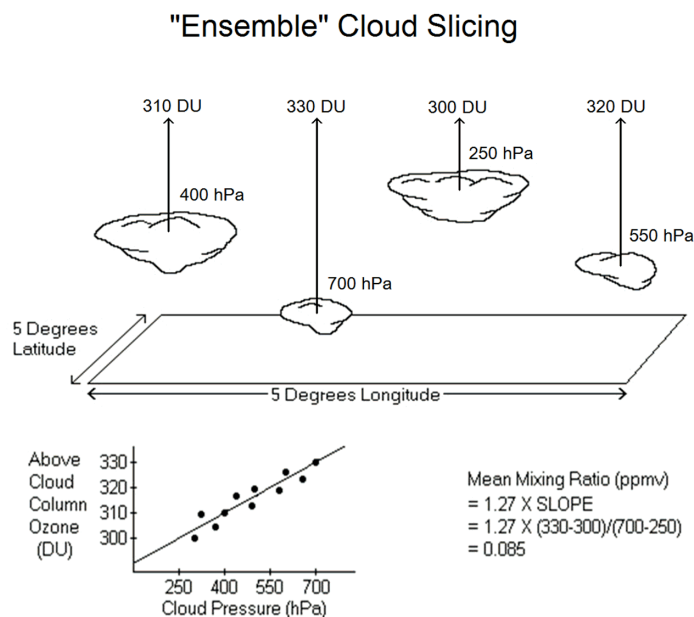


Figure 1. A schematic diagram illustrating the ensemble cloud slicing method involving coincident measurements of above-cloud column ozone (i.e., column ozone measured from the top of the atmosphere down to cloud pressure) and cloud pressure to measure mean volume mixing ratio (see text). For deep convective cumulonimbus clouds the cloud tops are near the tropopause and so the mean volume mixing ratio is primarily a measurement of average “in-cloud” ozone concentration. This figure was adapted from Ziemke et al. (2001). For our study all measurements are from OMI (i.e., OMI above cloud ozone versus OMI OCP).

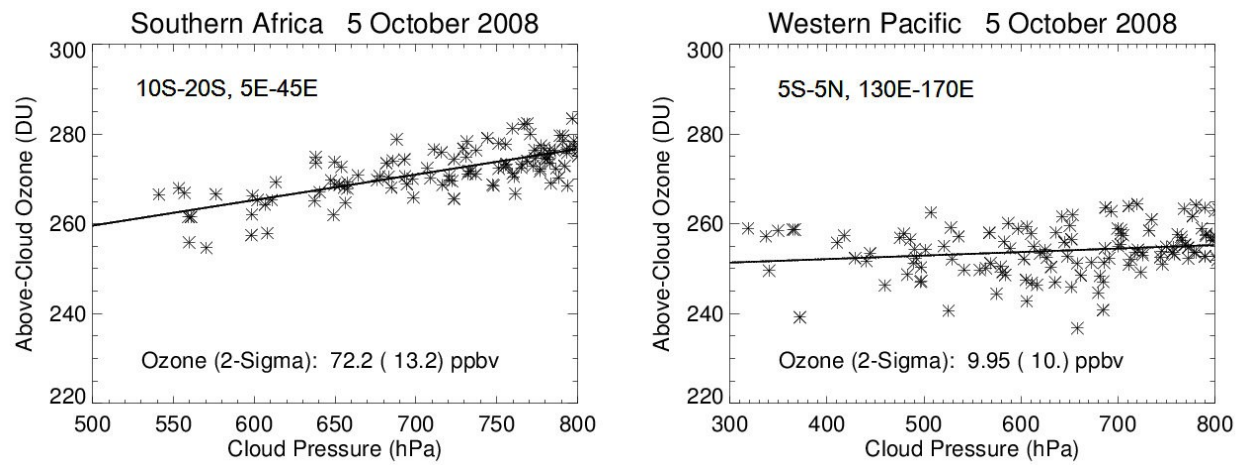


Figure 2. Examples of the ensemble cloud slicing technique using OMI measurements of above-cloud column ozone and cloud pressure (see text).

Tropospheric Column Ozone Measured Over Deep Convective Clouds

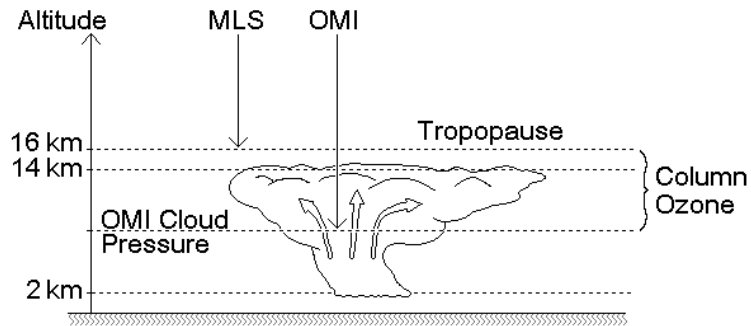


Figure 3. Schematic diagram of the OMI/MLS residual cloud slicing method. This depiction shows that deep convective clouds have OMI cloud optical centroid pressures (OCPs) lying deep inside the clouds with cloud tops often at tropopause level or very close to the tropopause. This figure was adapted from Ziemke et al. (2009).

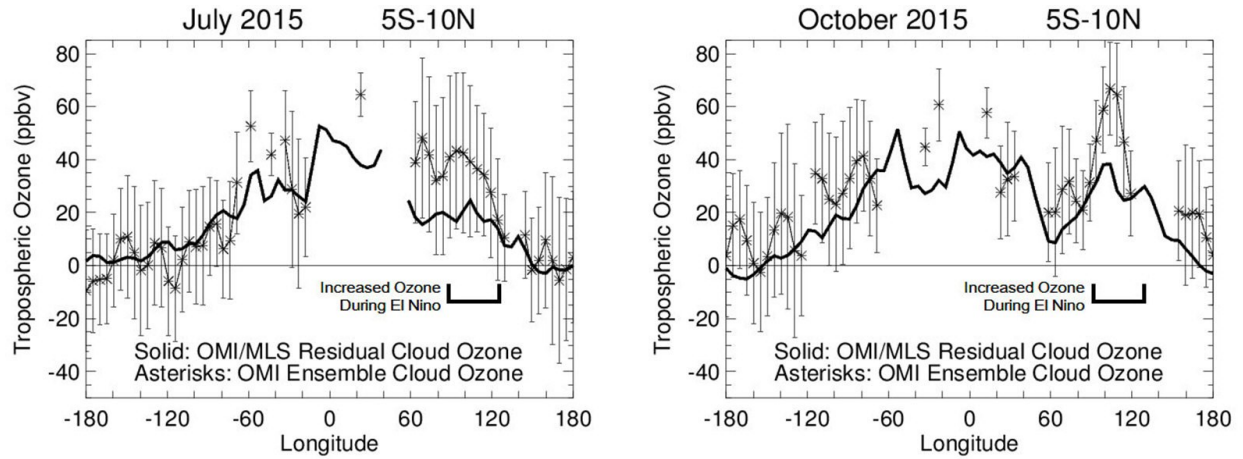


Figure 4. Comparisons of OMI/MLS (solid) and OMI ensemble (asterisks) cloud ozone VMR for July and October 2015 with both months coinciding with the intense 2014-2016 El Nino event. Measurements are averaged over the 5°S-10°N latitude band as a function of longitude (at 5° increments). The ensemble measurements include calculated $\pm 2\sigma$ uncertainties. Mean VMR for the ensemble measurements are calculated for all OCPs lying between 250hPa and 550 hPa and radiative cloud fractions $> 80\%$.

Cloud-Ozone Climatology

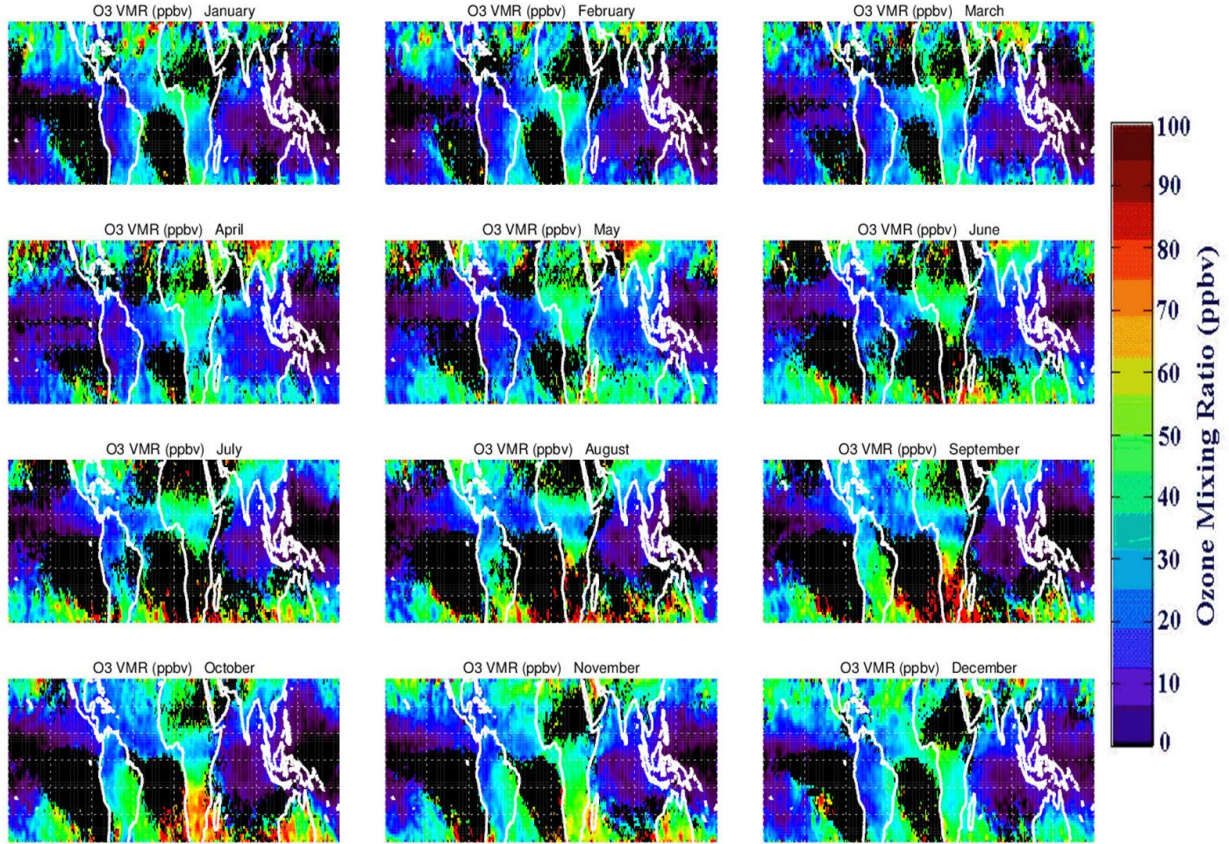


Figure 5. Monthly-mean climatology maps of OMI/MLS residual cloud ozone (units ppbv). Plotted is mean VMR representing average ozone concentration lying between the tropopause and OMI UV cloud pressure (OCP) as described in Section 3. The mean mixing ratio is calculated for OCPs varying between 250 hPa and 550 hPa. Black regions indicate not enough deep convective clouds present or mostly low clouds such as marine stratus clouds with OCP lying below the 550 hPa threshold.

Tropospheric Ozone Climatology

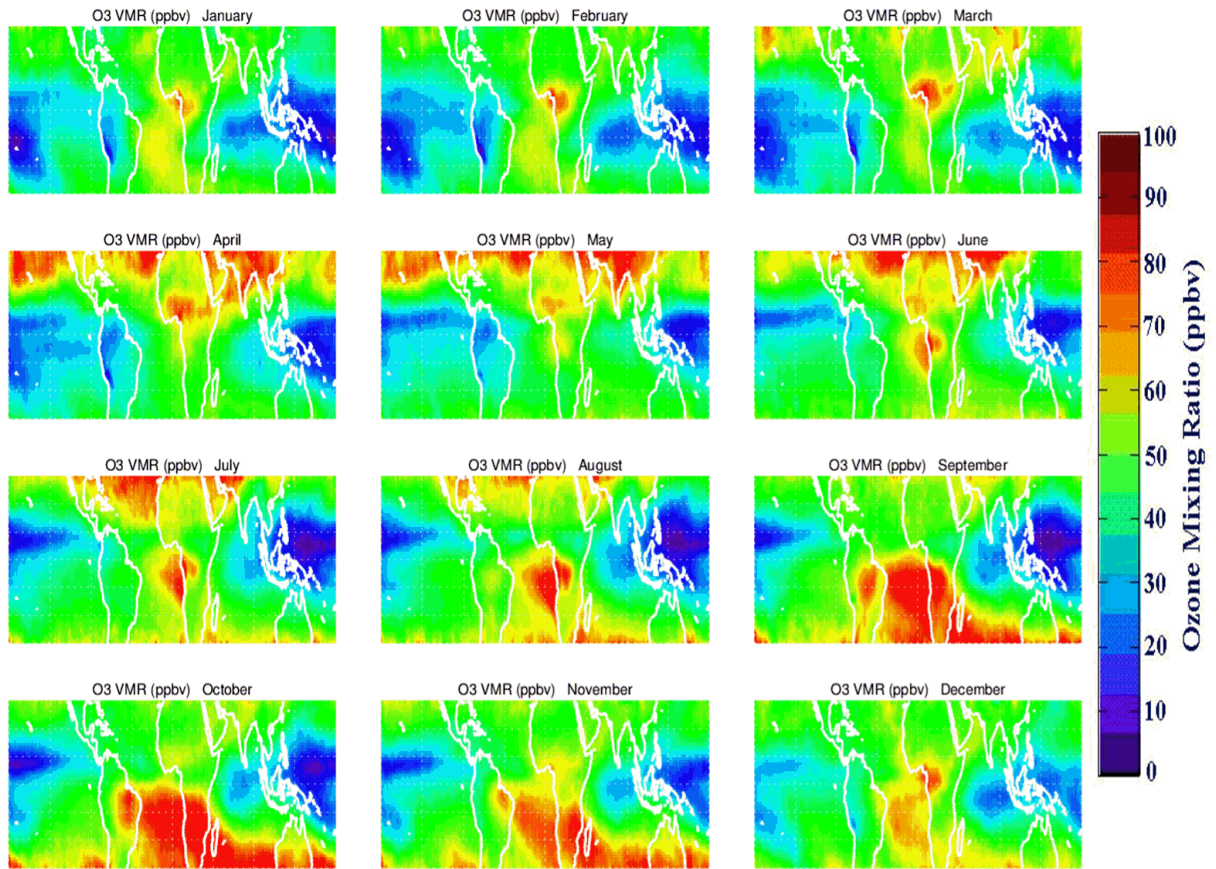


Figure 6. Similar to Figure 5, but instead plotting monthly-mean climatology maps of OMI/MLS VMR (units ppbv) for OMI near clear-sky scenes (i.e., radiative cloud fractions less than 30%).

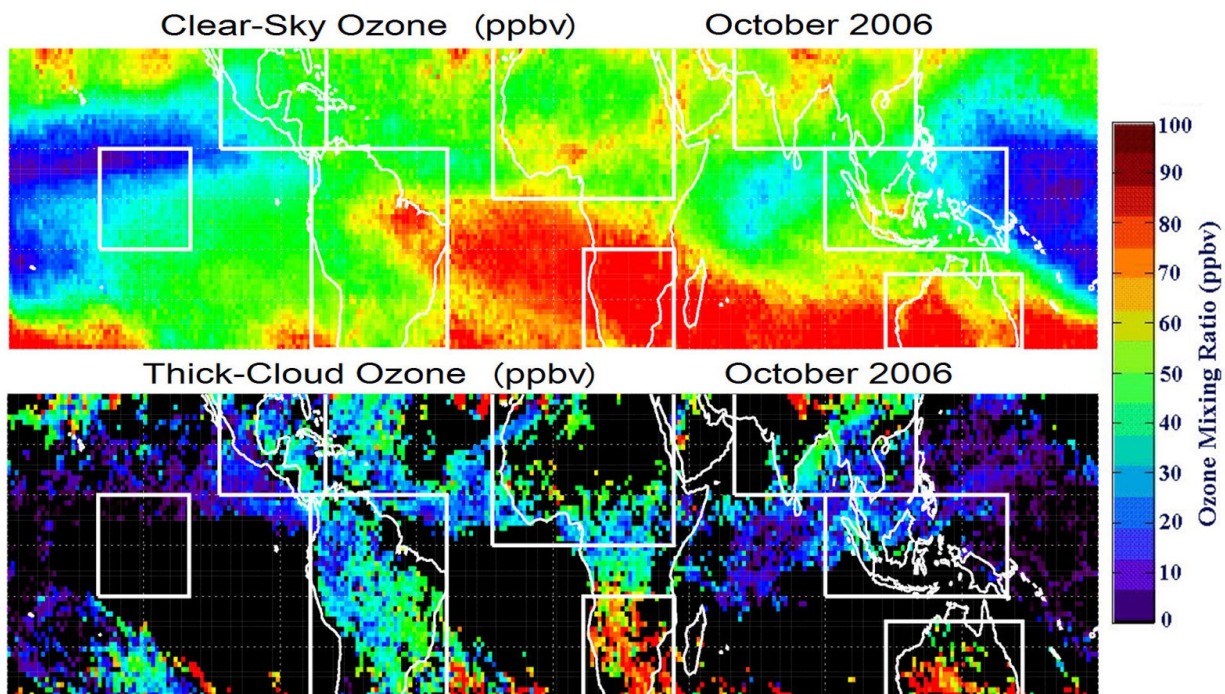


Figure 7. (Top) Background (near clear-sky) tropospheric ozone in units ppbv for October 2006. Shown as white rectangles are eight selected regions of interest where measurements are averaged each month to generate long record time series for October 2004 – April 2016. (Bottom) Same as top but instead for cloud ozone.

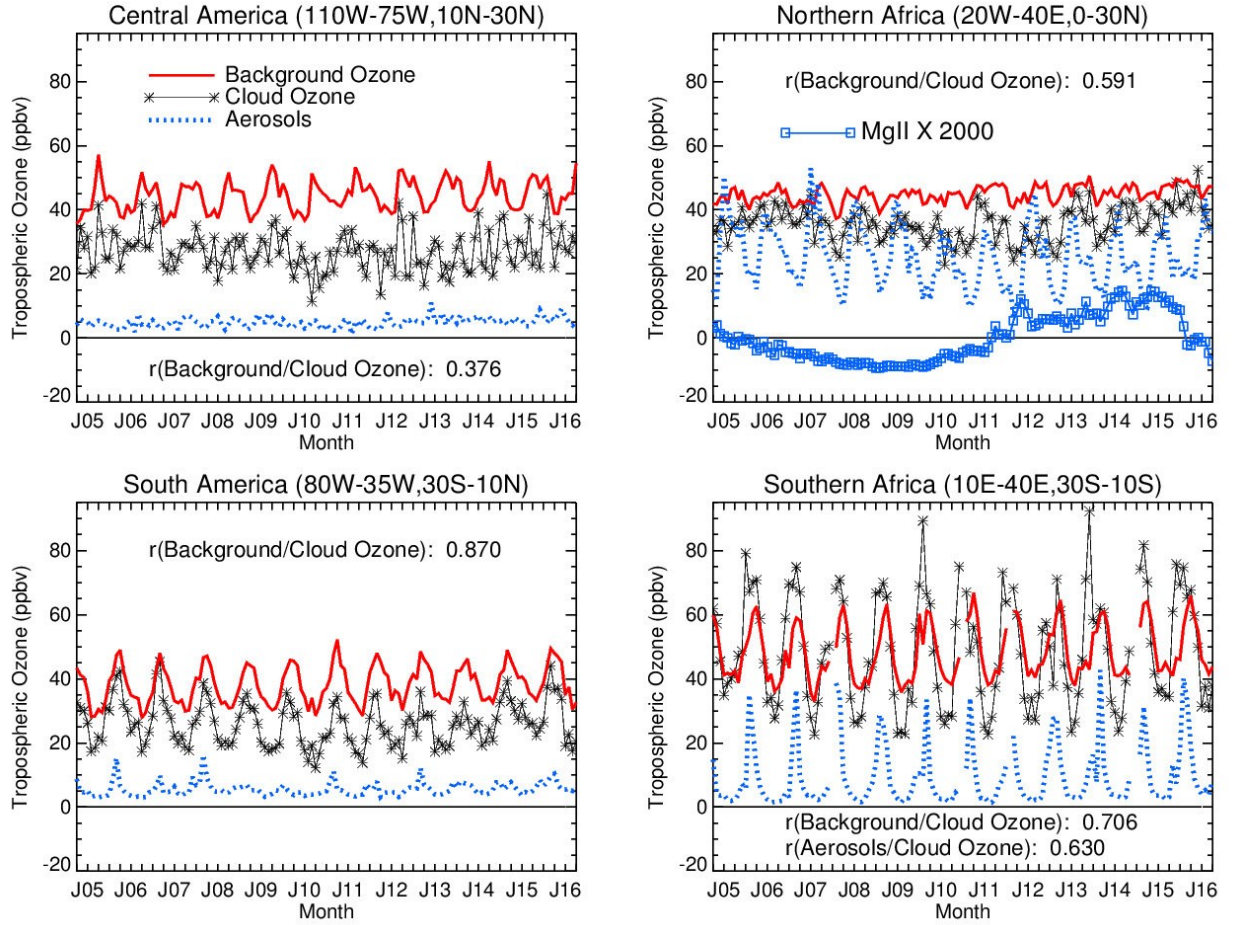


Figure 8. Monthly time series of background ozone (thick solid red curves) and cloud ozone (thin black curves with asterisks) for the regions of Central America, South America, northern Africa, and southern Africa in Figure 7. All ozone units are ppbv. Also shown for each of these landmass regions is the OMI monthly aerosol index time series (dotted blue curves, no units) which was re-scaled (i.e., multiplied by 60) for plotting. Included for the northern Africa region is the solar MgII index (SI units) that has been re-scaled for plotting (i.e., time average removed and then multiplied by 2000). The correlation between background ozone and cloud ozone is indicated in each panel. Also include for southern Africa is correlation between aerosol index and cloud ozone.

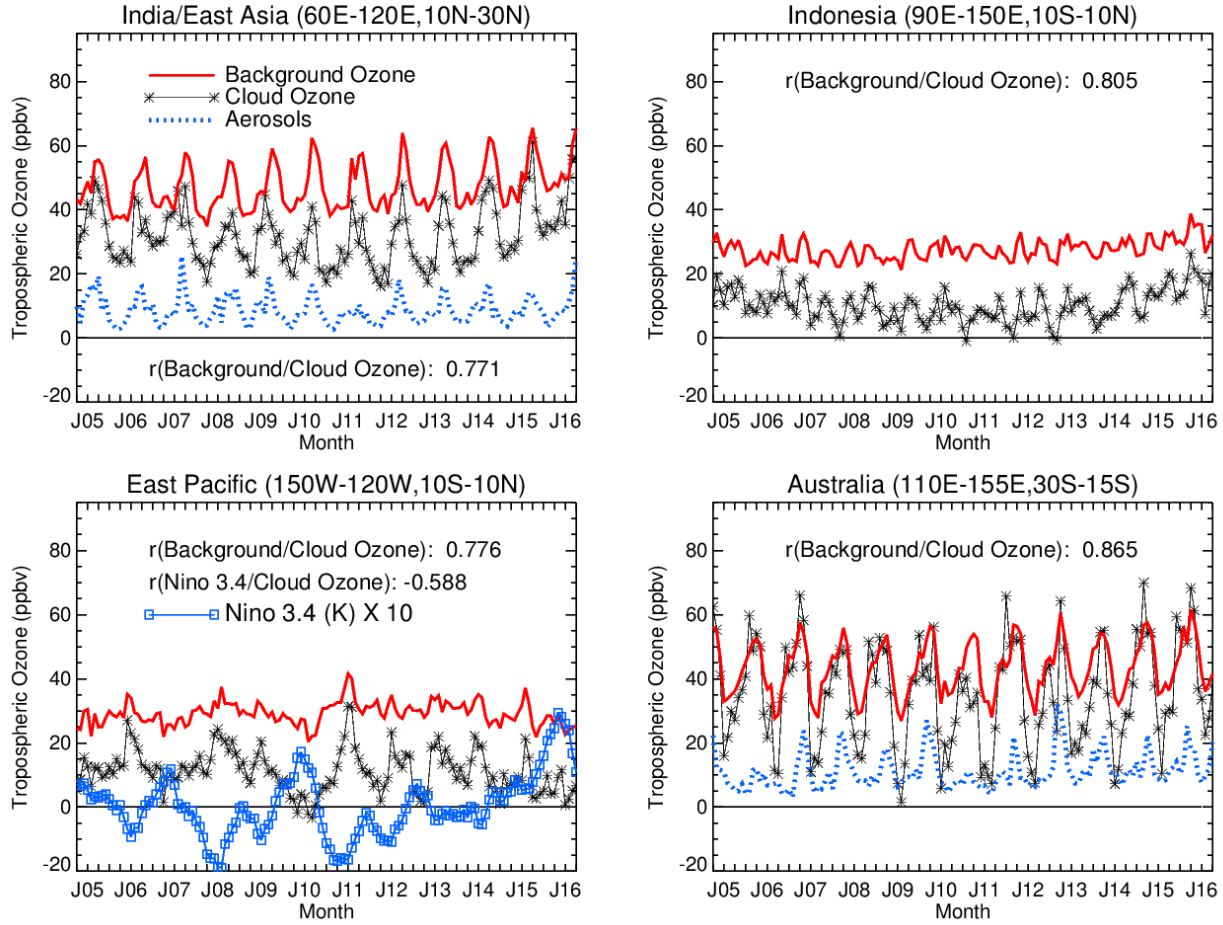


Figure 9. Similar to Figure 8, but instead for the regions of India/east Asia, Indonesia, eastern Pacific, and Australia. Aerosol index time series (dotted) for the landmass regions is again shown. Also included for the eastern Pacific (lower left panel) is the Nino 3.4 index (blue squares, units K) and its correlation with cloud ozone. The Nino 3.4 index was re-scaled (multiplied by 10) for plotting with ozone time series.

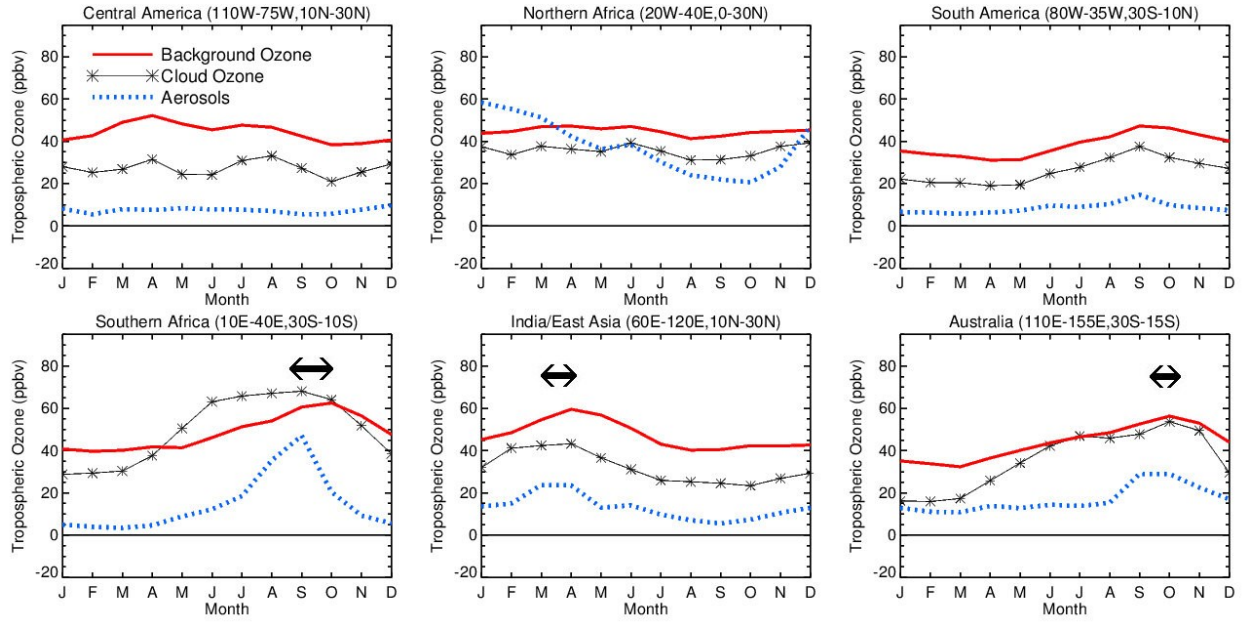


Figure 10. Twelve-month climatology time series for the six continental land-mass regions plotted in Figures 8 and 9 using the same color scheme. Shown here are background ozone (solid red curves), cloud ozone (asterisks), and aerosol index (dotted blue curves). The OMI aerosol index has been re-scaled (i.e., multiplied by 60) for plotting. Approximate phase shifts between background ozone and aerosol index time series are shown with dark arrows.